The influence of climatic and hydographic factors on growth of Engelmann spruce (*Picea engelmannii*) in the Senator Beck Study Area, Red Mountain Pass, San Juan Mountains, CO

David K. Scott

D. Scott (Corresponding author)
Department of Anthropology
B-219 Andrew G. Clark Building
Colorado State University
Fort Collins, CO 80523-1787
davidks@rams.colostate.edu
319-270-6768

Date of report draft: August 20, 2014

Purpose

Research was conducted to investigate relationships between tree growth and hydro-climate variables. This research was initiated in response to concerns that recent and future changes in climate may stress subalpine trees leading to weakened defensive capacity and greater susceptibility to outbreaks of native bark beetles. Specifically, there is special concern about outbreaks of native spruce bark beetle populations and the role that temperature, precipitation and snow-melt timing play in making trees susceptible to beetle attack.

Introduction

In recent years, trends of decreased snowpack accompanied by increased melt rate have been observed in the San Juan Mountains. These changes in the total volume and melt rate have been attributed to drier winters, warmer springtime temperatures and increased occurrence of "dust-on-snow" events (DOS) which occur when wind-driven dust originating from the desert Southwest is deposited on top of, or along with mountain snows. During DOS events, dust particles darken the otherwise reflective snow surface, decreasing its albedo and increasing the ratio of absorbed to reflected radiative energy. Though the mechanism by which DOS influences snowmelt is simple, the significance of particular DOS events is complicated by factors such as slope angle, aspect, terrain and vegetation shading, temperature and winds which interact with albedo-related forcing. The (indirect) effects of DOS on ecological communities and processes are also subject to the influence of topography (Steltzer et al. 2009), weather and shading.

This research in this report explores the influence of climo-hydrologic factors on a single component of a high elevation system, specifically, the health of treeline forests. Radial growth is used as a proxy for tree health. Variables relating to climate (precipitation, temperature), hydrography (snow-water equivalent, timing and rate of snow melt), forest stand structure (canopy closure), and tree-level dominance (canopy strata position) are used to the variability of radial growth within the study area. Two types of modeling approaches were used to explore linear and non-linear relationships in the data: linear models and random-forest prediction methods.

Methods

Sampling strategy

All sampling was done within the Senator Beck Basin (SBB) near Red Mountain Pass in the San Juan Mountains, CO (USA) operated by the Center for Snow and Avalanche Studies based in nearby Silverton. Our goal was to obtain samples from trees that show annual variations in radial growth related to snowpack variation and associated moisture stress. I sought to stratify sampling based on theory and experimental findings which suggest DOS effects might be greatest in areas with greater sun exposure. Half of the sampling (n = 63 trees) was conducted in heavily forested north-facing slopes and the other half (n = 58) on sparsely forested south-facing slopes.

Site selection

Eleven total sites were sampled within the study area. Samples were collected from trees on sites with relatively thin, rocky substrate in what appeared to be well-drained locations. Sites also had to have a minimum of 5 trees. Because forest cover on the southerly slopes was sparse, trees had to be sampled from numerous sites (n = 8) located in distinct clusters of trees. In contrast, moisture-sensitive sites were uncommon on north-facing slopes and as a result trees were sampled from only three sites.

Response variable – annual radial growth

The response variable data are measurements of annual radial growth (mm) collected from a total of 124 trees across 11 sites throughout the SBB. Two cores were extracted from opposite sides of each bole at knee to chest height. Increment core samples were then processed in a lab using standard dendrochronology techniques (Stokes and Smiley 1968). Because all samples were from live trees with a complete annual ring for the 2013 growth season dating individual series was straightforward and statistical cross-dating was unnecessary. However, I visually crossdated samples using identified marker years. No missing rings were identified in any of the samples. All samples were scanned to a digital image at 1200 dots per inch and then annual ring-widths during the period 1980-2013 were measured using ImageJ image analysis software (Abràmoff et al. 2004).

Most cores were extracted from chest height (50-90 cm) though small tree size, bole damage and wood rot required that some be extracted from as low as 15 cm and as high as 140 cm. While analyses revealed weak but statistically significant relationships between absolute ring width and core height magnitude (Figure 1; r2 = 0.01, p-value = 0.03) and variance (r2 = 0.03; p.value = 0.008), other variables such as tree diameter (Figure 1; $r^2 = 0.15$; p.value < 0.001) and crown position (Figure 1; $r^2 = 0.30$; p.value < 0.001) were found to correlate more strongly with ring width. Furthermore, when ring width was modeled using all three of these variables, core height was no longer a significant predictor of ring width (p.value = 0.48). I find no reason to believe that the variation in coring heights among our samples is responsible for trends in the ring width data.

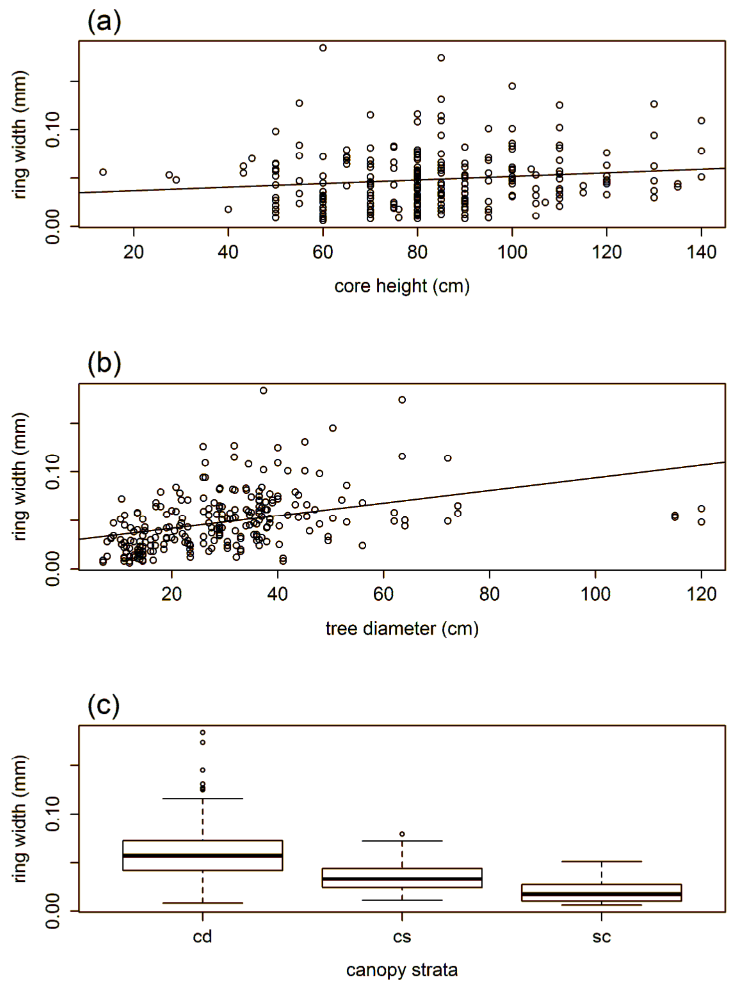

Figure 1 -Radial growth (year 1985 shown as an example) as a function of increment coring height (a), tree diameter (b), and canopy strata (c). Data shown are from 248 cores from 124 Engelmann spruce trees near treeline in the Senator Beck Basin, San Juan Mountains, CO. The relationship between ring width and core height is relatively weak with a large amount of unexplained variance. Canopy strata classes are as follows: canopy dominant (cd); canopy sub-dominant (cs); sub-canopy (sc). These categories indicate the relative position of each tree in the local forest structure.

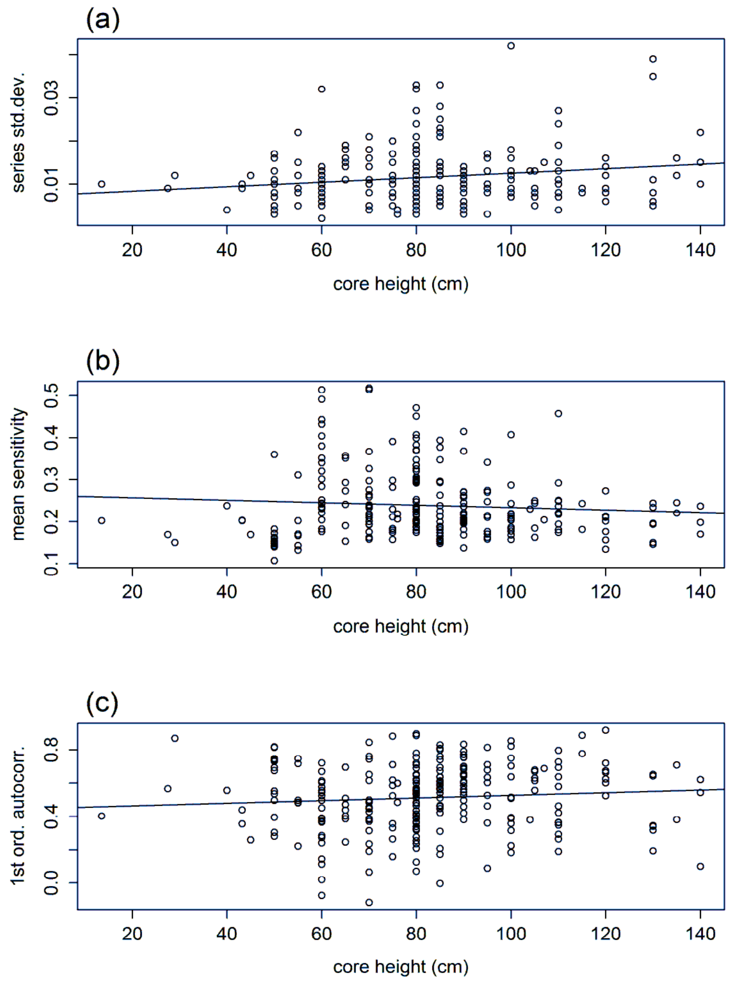

Figure 2 - The relationship between core height and ring-width series standard deviation (a), mean sensitivity (b), and first-order autocorrelation (c). Data shown are from 248 cores from 124 Engelmann spruce trees near treeline in the Senator Beck Basin, San Juan Mountains, CO. All relationships involving core height are relatively weak with a large amount of unexplained variance.

Independent variables

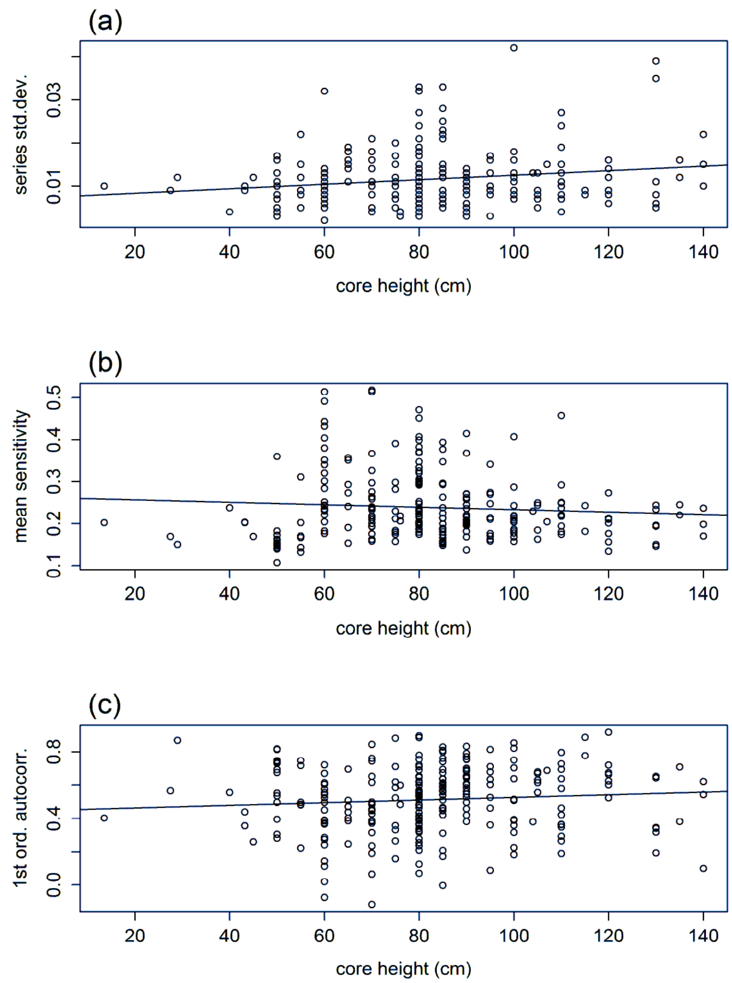

Stand structure and tree position

Figure 2 - The relationship between core height and ring-width series standard deviation (a), mean sensitivity (b), and first-order autocorrelation (c). Data shown are from 248 cores from 124 Engelmann spruce trees near treeline in the Senator Beck Basin, San Juan Mountains, CO. All relationships involving core height are relatively weak with a large amount of unexplained variance.

Independent variables

Stand structure and tree position

Forest cover within the SBB is highly variable in terms of stand age, density, structure and canopy cover. Though aging stands and calculating canopy cover were beyond the scope of this study, I attempted to account for differences in forest structure and position using two subjectively measured categorical variables: canopy structure and canopy position. I visually assessed and recorded the forest canopy structure surround each tree using the following classification:

Table 1 - Forest canopy structure classification used in this study. See Figure 3 for illustration.

Canopy Structure	Description
Totally closed canopy (TCC)	Only canopy dominant trees receive full sun exposure. Tall, dominant overstory trees are close to one another with significant touching and overlap. This forest casts significant shade on sub-dominant and sub-canopy trees.
Partially closed canopy (PCC)	Canopy dominant trees receive full sun. Sub-dominants and sub-canopy trees receive partial to limited full sun exposure. Same as TCC (above), but with fewer dominant overstory tree canopies touching. Significant gaps in the overstory allow direct light to reach both sub-dominant and sub-canopy trees.
Lower closed canopy (LCC)	Canopy dominant trees receive full sun. Sub-dominant trees receive limited full sun exposure. Sub-canopy trees are shaded. Same as PCC (above), but with a dense layer of canopy sub-dominant trees that shade sub-canopy trees.
Open canopy (OC)	Trees of all sizes receive full sun for much of each day.

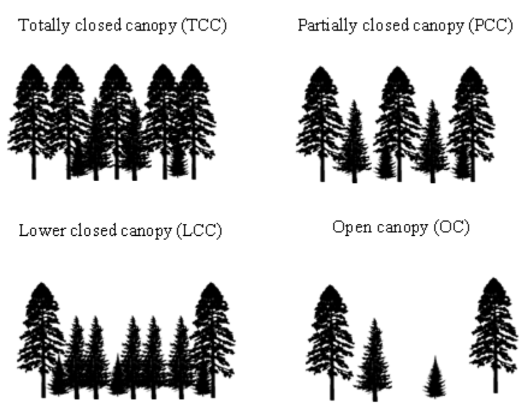

Figure 3 - Illustration showing canopy structure classifications used in this study. For a description see Table 1.

We also visually subjectively classified the position of each sampled tree's crown within the surrounding forest canopy using the following classification:

Table 2 - Tree crown position classification used in this study. See Figure 4 for illustration.

Crown Position	Description
Canopy dominant **(CD)**	The largest, tallest trees in the stand that receive full sun all day with limited shading from surrounding trees
Canopy sub-dominant **(CS)**	Trees whose crowns are positioned within a secondary canopy strata and that receive partial shading from canopy dominants
Sub-canopy **(SC)**	Smaller trees whose crowns are positioned below canopy sub-dominants and receive significant shading from surrounding forest.

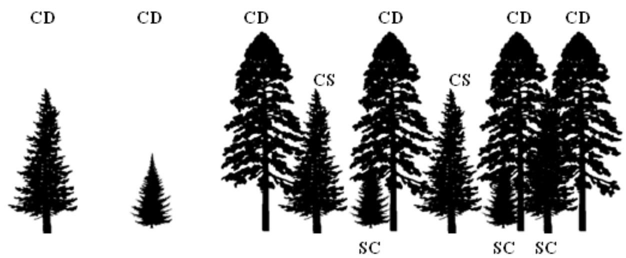

Figure 4 - Illustration showing crown position classes used in this study. Classes include canopy dominant (CD), canopy sub-dominant (CS), and sub-canopy (SC) trees. For a description see Table 2.

Hydro-climate variables

We compiled monthly temperature, precipitation and annual snow water equivalent data for water years 1980-2013. Water years are defined as the period October through September of the following year. Annual radial growth typically begins late-spring and ends late-summer.

The SBB is home to two heavily-instrumented weather and snow-hydrology measurement stations. However, the data for these stations begins in 2005, which is not a long enough record for a robust analysis using tree ring data. A nearby SNOTEL station (National Resource Conservation Science site # 713) on Red Mountain Pass has records extending back to 1980 and the annual snow water equivalent data from this station was easily obtained using the SNOTEL data portal (http://www.wcc.nrcs.usda.gov//). However, for temperature and precipitation, monthly statistics would have had to be compiled from the raw dataset which is complicated by missing data. A far easier approach was to obtain temperature and precipitation data from the spatially and temporally complete PRISM datasets (http://www.prism.oregonstate.edu/) which uses algorithms to interpolate temperature and precipitation across topographically complex topography using data from nearby weather stations, including SNOTEL stations. Data covering the SBB were extracted from the PRISM website using the following coordinates: Longitude = -107.71007, Latitude = 37.90754. Monthly precipitation data from PRISM and the SBB Swamp Angel station are very similar in magnitude (Figure 5; Pearson's r^2 = 0.93).

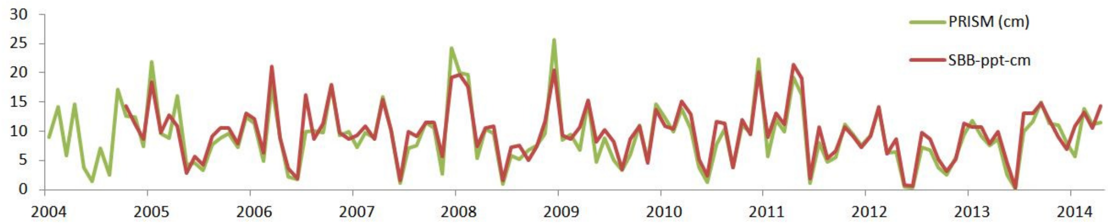

Figure 5 - Precipitation time series data for the Senator Beck Basin Study area, CO. Data from the interpolated PRISM climate dataset (green) and the station-based data from the Swamp Angel weather station (red) operated by the Center for Snow and Avalanche Studies are shown. These two data sets are strongly correlated (Pearson r^2 = 0.93).

Dust-on-snow data

Techniques to study the deposition of dust onto snowpack and related effects on snowpack albedo are rapidly evolving and improving. The Colorado Dust-on-Snow program (CODOS) of the Center for Snow and Avalanche Studies began rigorous dust-on-snow monitoring with the establishment of the Senator Beck Basin Study Area in 2003. Since the winter of 2003/2004, 91 separate dust events have been documented at SBB (CODOS, 2014). Although that period of record coincides with regional increases in dust deposition (Brahney et al, 2013), no prior dust-on-snow monitoring preceded CODOS, limiting our ability to assess the impact of such events on forest conditions at SBB. Nonetheless, this decade-long period of increasing dust-on-snow frequency and intensity at SBB has substantially altered the timing and rates of snowmelt with the general effect of accelerating the loss of snowcover, as compared to the modeled loss of snowcover in the absence of dust in the snowpack (Skiles et al, 2012).

In the absence of a longer period of record of DOS and albedo data, I used metrics associated with snowpack and DOS effects to discern the influence of snowpack quantity and melt timing on annual radial growth in trees.

Table 3 - Snowpack water-year descriptive metrics used in this study

Canopy Type	Description
Maximum water year SWE (swemx_in)	The maximum snow-water equivalent in inches
Date of maximum SWE (swemx_doy)	The ordinal date (range: 1-365) during which *swemx_in* occurred.
Snow all gone date (sag_doy)	The ordinal date that SWE was measured as zero for the first time during the water year.
Melt period **(melt_per)**	The number of days between the date of maximum SWE and the snow-all-gone date. Calculated as: *melt_per = sag_doy - swemx_doy*

Specifically, I calculated the melt period and snow-all-gone date and then attempted to model these variables using other hydroclimatic variables (eg. temperature, precipitation, peak SWE date) as predictors. The residual error from these models should include the influence of DOS on snowmelt. I used Random Forest models to explore the importance of predictor variables and fit variables with non-linear relationships. Linear models were built using backward stepwise variable selection and Akaike's Information Criterion.

Results & Discussion

Radial growth and sensitivity of sampled trees

Mean radial growth

Radial growth was greatest in canopy dominant trees regardless of the canopy structure of the surrounding forest. Radial growth was especially large in forest with an open canopy structure. This difference could be due to either the decreased competition in open canopy forest sites or because of differences in tree age. Tree-aging and calculations of basal area increment would be needed to further elucidate such a difference and was beyond the scope of the present study.

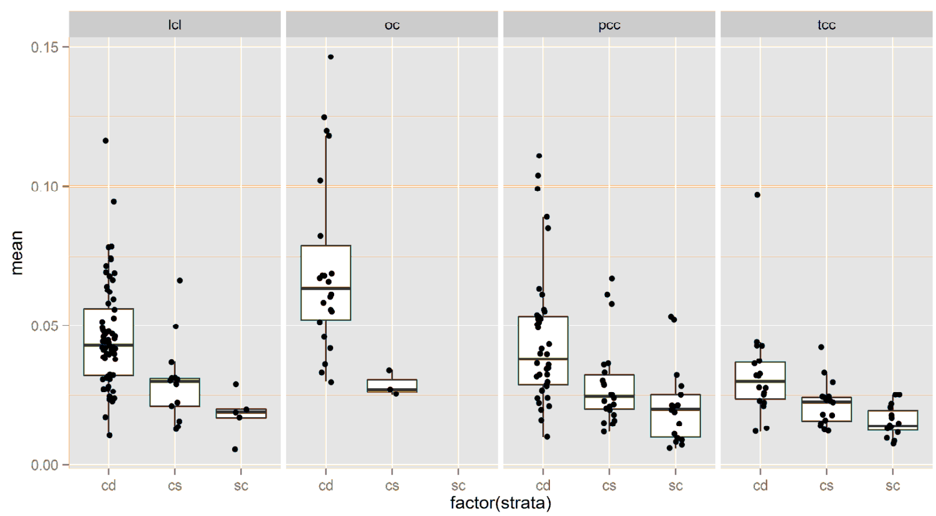

Figure 6 – Boxplots of mean radial growth (y axis) by tree position (x axis) and forest canopy type (panels). Boxplots show the mean (dark bar), 2nd and 3rd quartiles (white box) and 1.5 times the interquartile range (whiskers). Points are "jittered" for clarity and all points beyond the wiskers are outliers. The four panels group data into the following canopy structure classes: lower closed canopy (lcl); open canopy (oc); partially closed canopy (pcc); totally closed canopy (tcc). Columns within panels group data according to the canopy position of individual trees: canopy dominant (cd); canopy sub-dominant (cs); sub-canopy (sc).

Tree-ring sensitivity

Mean sensitivity varied little within and among the open canopy, partially closed canopy, and totally closed canopy groups. The lower closed canopy group showed elevated sensitivity among canopy sub-dominant and sub-canopy trees, though the sample size for sub-canopy trees is very small. Stands with a lower closed canopy structure appeared to be the most densely forests stands, though this density was only observed and not quantified in the field. This increased sensitivity might be explained by more intense competition in stands with a lower closed canopy and greater tree density.

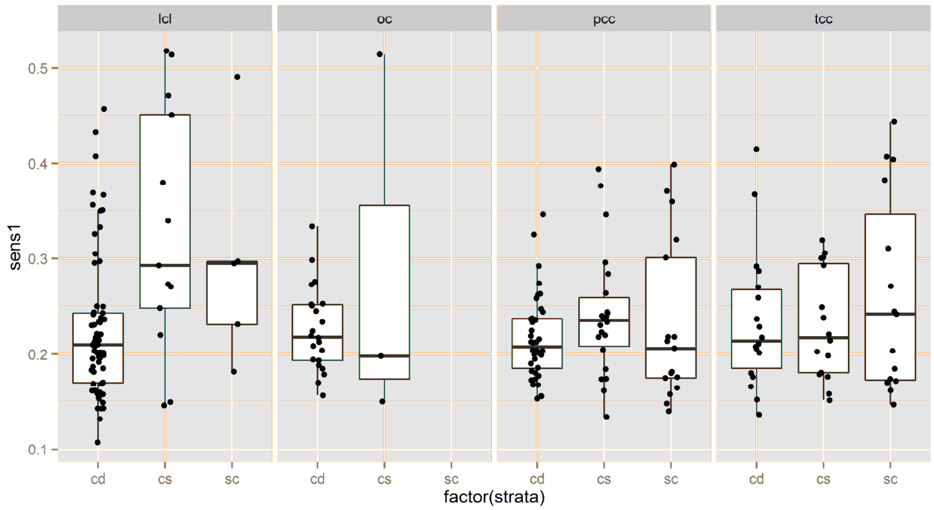

Figure 7 – Boxplots showing the distribution of tree-ring sensitivity (y axis) by tree position (x axis) and forest canopy type (panels). Boxplot construction and panel and columns groupings are the same as Figure 6.

Dust on snow metrics

We hypothesize that DOS events affect forest health through seasonal water availability. Faster melting of snowpack might result in more acute and persistent pre-monsoon moisture stress. Because many trees exhibit decreased radial growth during years of severe moisture stress, it may be possible to find evidence of DOS effects in tree ring series.

The *ideal* way to correlate tree growth with DOS effects would be to use a data set that captures the true effect of DOS on snowmelt. While significant progress has been made modeling the effect of DOS, the available data do not extend far enough backwards in time for robust correlation. In the absence of long-term datasets for dust accumulation or snow surface albedo, I used the snow-melt period (SMP) and snow-all gone (SAG) date. The metric SMP is the number of days separating the dates of maximum SWE and SAG. The metric SAG is defined as the date during which SWE reaches zero for the first time since the date of maximum SWE. With increased DOS effects, SAG is expected to occur earlier and SMP expected to be shorter.

Year-to-year differences in SAG and SMP are not due solely to DOS effects. Other factors such as total SWE, timing of peak SWE, cloud cover, temperature and humidity also play roles in the melting of snowpack. To better understand the nature and variability of SAG and SMP, I modeled them using hydroclimate variables.

Melt Period

During the 1981-2013 period, SMP varied between 26 and 67 days, with a mean of 45. The distribution of these data shows a skew towards longer periods.

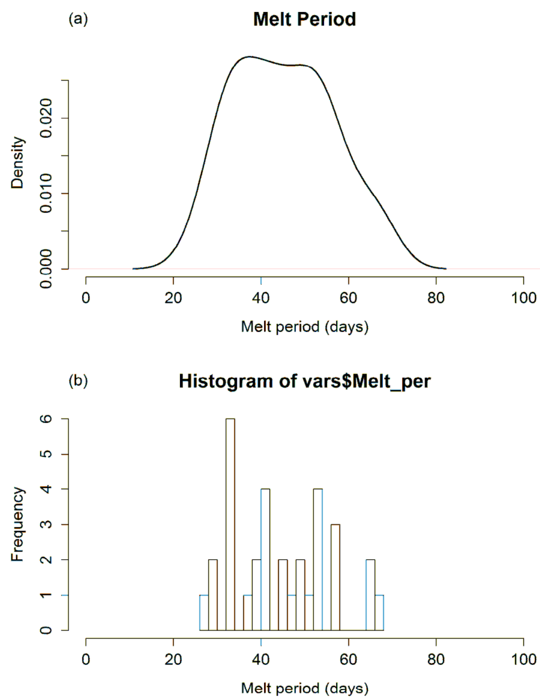

Figure 8 - Distribution of the melt period (melt_per) data. These data are derived from metrics of peak SWE and snow-all-gone dates acquired from the SNOTEL station #713 on Red Mountain Pass in the San Juan Mountains, which is very near the SBB (2 km south of Swamp Angel Study Plot, at similar elevation). Specifically, the melt period is difference between the snow-all-gone date and the peak SWE date. Data shown are for the 32 water years between 1981- 2013.

We checked the relationships between snowmelt period and its constituent metrics, peak SWE date (swemx_doy) and snow-all-gone date (sag_doy), as well as the max SWE (swemx_in) which ought to play an important role in how long it takes for the snowpack to ablate. I found melt period (melt_per) to be most strongly correlated with *swemx_doy* (Figure 9), which explained 35% of the variance. The melt period is more strongly related to the timing of the SWE peak than to either the disappearance of SWE or the total amount of SWE.

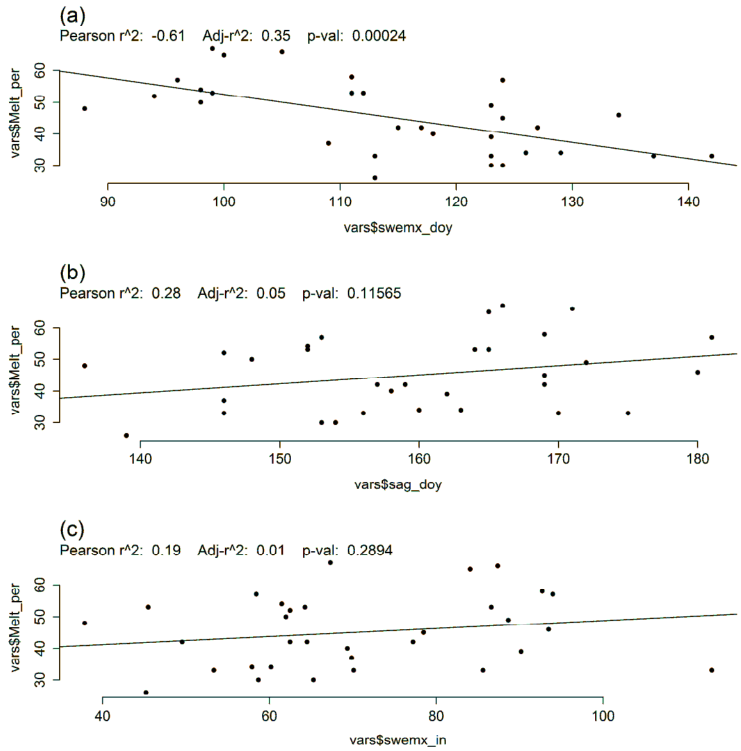

Figure 9 - Scatter plots showing the snow-melt period (melt_per; y axis) as a function of SWE max day-of-year (a), snow all gone day of year (b), and SWE max in inches (c).

A look at the distribution sag_doy and swemx_doy helps explain this relationship. Whereas the snow-all-gone data are strongly unimodal (centered on the first week of June), peak SWE is more complex and shows a somewhat bi-modal distribution with (at least) two peaks, one near the first week of April and one or two others near late April and early May. Whereas the snow-all-gone data has a strong central tendency, the peak SWE date has several central tendencies which may be related to recurring weather patterns (wet springs versus dry springs) that perhaps represent the influence of atmospheric teleconnections (ENSO, AMO). For the purposes of this study, it was sufficient to discover and understand the important role the peak SWE date plays on the melting period.

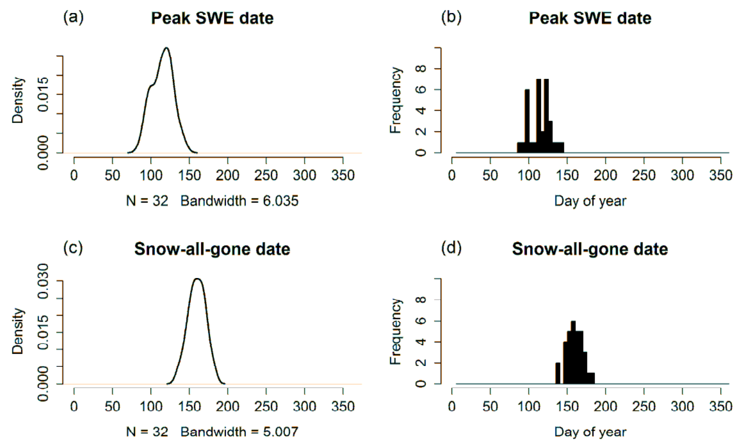

Figure 10 – Kernel density plots and histograms showing the data distributions for swemx_doy (a and b) and sag_doy (c and d). Ordinal days are presented. Snow-water equivalent data from which these data were derived come from the Red Mountain Pass SNOTEL station #713 and are for the 32 water years between 1981-2013. Histogram bars are five day intervals. For reference, ordinal days 100, 150, and 200 correspond with April 10th, May 30th, and July 19th, respectively

I continued building the model of melt period by fitting variables to the residual error. I excluded the variable *sag_doy* from further consideration because it along with *swemx_doy* would result in a perfect fit with no unexplained variance because these are the exact data used to derive the melt period data. A Random Forest model run of the residuals from this linear model indicate that both *swemx_in* and *ppt.05* are important predictors of the residual error from the initial model. These two variables also happen to be strongly collinear. Water years with exceptionally high SWE are often characterized as having many late-season storms. Furthermore, storms occurring in May generally bring very dense snows contributing large additional SWE to the existing snowpack. Given the collinearity and underlying meteorologic mechanisms, I chose swemx_in since it would capture both the seasonal precipitation along with any May precipitation specifically.

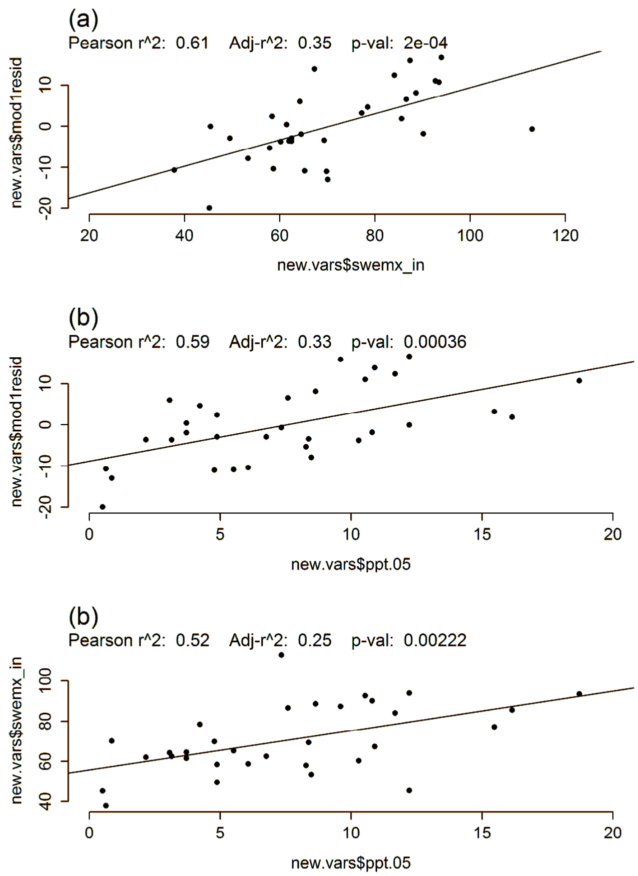

Figure 11 - Scatterplot showing the residuals from the original model (melt_per ~ swemx_doy) as a function of water year maximum SWE (*swemx_in*; a) and total May precipitation (*ppt.05*; b). The strong correlation between *swemx_in* and *ppt.05* is also shown (c).

Backward step-wise variable selection using AIC criteria and a subset of predictors resulted in a model with three variables significant at the $p < 0.001$ level (swemx_doy, swemx_in, ppt.05), two at the $p < 0.05$ level (ppt.06, tmean.06) and one variable significant at the $p < 0.1$ level (ppt.12p).

Table 4 - Model variable subsets for use in stepwise variable selection.

Variable name	Variable description	Melt_per	sag_doy	chron
Year	Represents a trend in the data	X	X	X
swemx_in	Max SWE (in)	X	X	X
swemx_doy	SWE max day-of-year	X	X	X
sag_doy	Snow-all-gone day-of-year			X
Melt_per	Snowmelt period beginning swemx_doy			X
swemx_in.p	Max SWE (in), previous water year			X
swemx_doy.p	SWE max day-of-year, previous water year			X
sag_doy.p	Snow-all-gone day-of-year, previous WY			X
Melt_per.p	Snowmelt period, previous WY			X
ppt.01p	January precipitation, previous calendar year			X
ppt.02p	February precipitation, previous calendar year			X
ppt.03p	March precipitation, previous calendar year			X
ppt.04p	April precipitation, previous calendar year			X
ppt.05p	May precipitation, previous calendar year			X
ppt.06p	June precipitation, previous calendar year			X
ppt.07p	July precipitation, previous calendar year			X
ppt.08p	August precipitation, previous calendar year			X
ppt.09p	September precip., previous calendar year			X
ppt.10p	October precipitation, previous calendar year	X	X	X
ppt.11p	November precip., previous calendar year	X	X	X
ppt.12p	December precip., previous calendar year	X	X	X
ppt.01	January precipitation, current calendar year	X	X	X
ppt.02	February precip.	X	X	X
ppt.03	March precip.	X	X	X
ppt.04	April precip.	X	X	X
ppt.05	May precip.	X	X	X
ppt.06	June precip.	X	X	X
ppt.07	June precip.	X	X	X
ppt.08	June precip.			X
ppt.09	June precip.			X
tmean.01p	January mean temperature, previous cal. year			X
tmean.02p	February mean temperature, previous cal. year			X
tmean.03p	March mean temperature, previous cal. year			X
tmean.04p	April mean temperature, previous cal. year			X
tmean.05p	May mean temperature, previous cal. year			X
tmean.06p	June mean temperature, previous cal. year			X
tmean.07p	June mean temperature, previous cal. year			X
tmean.08p	June mean temperature, previous cal. year			X
tmean.09p	June mean temperature, previous cal. year			X
tmean.10p	June mean temperature, previous cal. year			X
tmean.11p	June mean temperature, previous cal. year			X
tmean.12p	June mean temperature, previous cal. year			X
tmean.01	January mean temperature, current cal. year	X	X	X
tmean.02	February mean temperature, current cal. year	X	X	X
tmean.03	March mean temperature, current cal. year	X	X	X
tmean.04	April mean temperature, current cal. year	X	X	X
tmean.05	May mean temperature, current cal. year	X	X	X
tmean.06	June mean temperature, current cal. year	X	X	X
tmean.07	June mean temperature, current cal. year	X	X	X
tmean.08	June mean temperature, current cal. year	X	X	X
tmean.09	June mean temperature, current cal. year	X	X	X

With the explanatory variables standardized (centered about the mean and scaled to one standard deviation), the relative strength (coefficient value) of each variable indicates that the peak SWE date is roughly twice as important as the peak SWE amount and roughly four times more important than June temperature (Table 5). The negative coefficient from peak SWE day of year indicates that a later peak SWE date results in a shorter SMP. The positive coefficients for *swemx_in* and *ppt.05* suggests that more SWE and more May precipitation results in a longer SMP. In contrast, the negative coefficient for June precipitation on the snowmelt period indicates that increased precipitation during June corresponds with shorter snowmelt periods—perhaps due to rain on snow effects. December precipitation (previous year, same water year) is also negatively associated with SMP, but this relationship is the weakest of the AIC selected variables and it is difficult to explain why increased December precipitation should result in a shortened SMP.

Table 5 - Standardized coefficients for the best model describing melt period.

Variable	Coefficient estimate	Coef. Std. Error
swemx_doy	-1.000	0.090
swemx_in	0.518	3.970
ppt.05	0.359	0.0914
tmean.06	-0.236	0.104
ppt.06	-0.212	0.0878
ppt.12p	-0.155	0.0897

Agreement in the direction of the effect of *swemx_in* and *ppt.05* further supports exclusion of the variable *ppt.05* on grounds of collinearity. In contrast, the opposite relationship between swemx_in and *ppt.06* suggests that the effect of the later is fundamentally different from that of the former and that *ppt.06* should be retained in the model, despite collinearity.

Table 6 - Performance metrics for models describing melt period. Models with lower AIC values are more informative (ie. better).

Model	adj. r^2	AIC
swemx_doy, swemx_in, ppt.05, tmean.06, ppt.06, ppt.12p	0.84	195.12
swemx_doy, swemx_in, ppt.05, ppt.06, tmean.06	0.83	196.72
swemx_doy, ppt.05, tmean.06, ppt.06, ppt.12p	0.75	208.76
swemx_doy, swemx_in, tmean.06, ppt.06	0.73	210.93
swemx_doy, swemx_in	0.65	216.78

The full, AIC-selected model explains 84% of the variability in the melt period data for the period 1981-2012 (Figure 12). More parsimonious models (Table 6) excluding collinear variables reduce the fit significantly, though they still explain much of the variability. Retaining collinear variables, such as swemx_in and ppt.05 could be justified since precipitation falling in May might have a disproportionate affect on increasing the length of the melt period and thus deserve greater weight in the model not captured by the swemx_in variable alone.

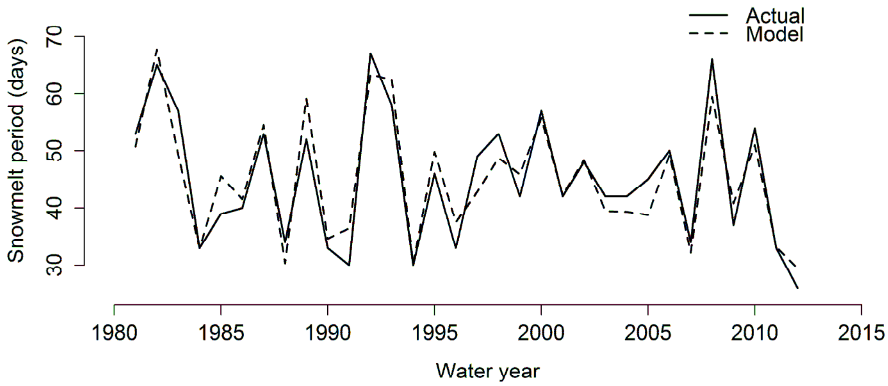

Figure 12 - Actual (solid) and modeled (dashed) snowmelt period (SMP) for the study area. The model was fit and variables selected using backwards stepwise least squares regression. The final model uses the following explanatory variables: swemx_doy, swemx_in, ppt.05, tmean.06, ppt.06, ppt.12p.

Snow-all-gone

Because the melt period and snow-all-gone are related metrics, I expect hydroclimatic variables explaining either one to be similar. Stepwise regression explaining SAG produced a list of important explanatory variables identical to that for SMP. Variable importance in a Random Forest model showed important differences.

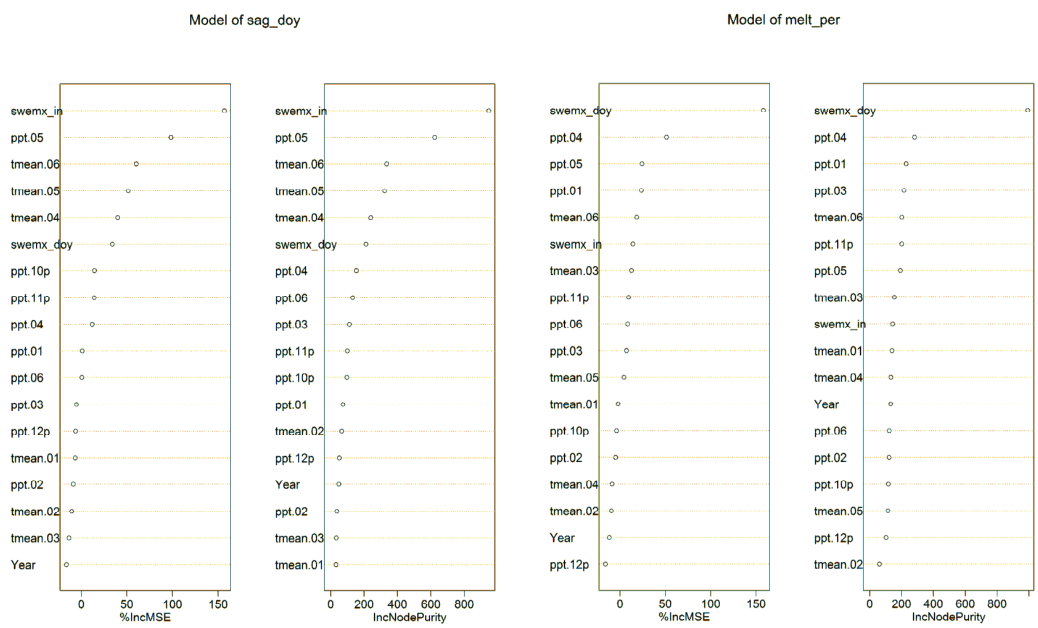

Figure 13 - Variable importance ranking output from a Random Forest model of snow-all-gone date for Red Mountain Pass, CO, USA. Data are from the period 1981-2012

Unlike the model of SMP, no single hydroclimatic variable overwhelmingly explained year-to-year variability in SAG dates. In fact, the timing of peak SWE (swemx_doy), which was overwhelmingly the most important variable explaining year-to-year variability in SMP, was much less important than other hydroclimatic variables in explaining SAG. Variables representing mean spring season monthly precipitation and temperatures were generally ranked as more important in the Random Forest model for SAG compared with the model of SMP.

Table 7 - Standardized coefficient estimates for linear model of snow-all-gone date (SAG).

Variable	Coefficient estimate	Coef. Std. Error
swemx_in	0.525	0.132
ppt.05	0.364	0.093
tmean.06	-0.240	0.105
ppt.06	-0.215	0.089
swemx_doy	0.191	0.091
ppt.12p	-0.157	0.091

The full, AIC-selected model explains 84% of the variability in the snow-all-gone data for the period 1981-2012, the same fit as the SMP model. Variable importance rankings and patterns of collinearity are also similar.

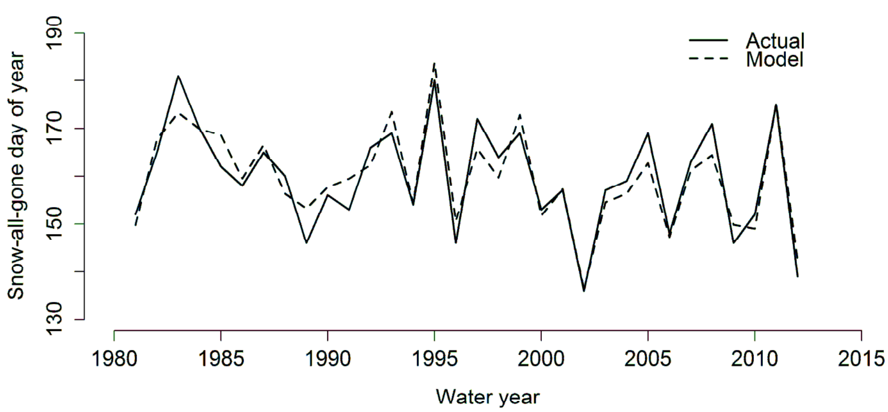

Figure 14 - Actual and modeled snow-all-gone date for the study area. The model was fit and variables selected using backwards stepwise least squares regression. The final model uses the following explanatory variables: swemx_doy, swemx_in, ppt.05, tmean.06, ppt.06, ppt.12p

Relationships between tree growth and hydroclimatic variables

Models of annual growth in trees as a function of hydroclimatic variables were constructed for all trees and for selected crown position and canopy structure subsets. Subsets of trees were selected based on importance to outbreak dynamics as well as sensitivity metrics (see *Radial growth and sensitivity of sampled trees*, above).

Table 4. In addition, a variable representing unexplained error from the full SMP model SAG model (*mod7resid*) was included. The inclusion of this variable introduces variability in snow-all-gone date not explained by the most important hydroclimatic explanatory variables and potentially due to the influence of DOS.

Subset	Which trees	Why selected
All trees	All trees sampled	Whole forest signal is a useful benchmark
Most sensitive trees	Canopy subdominants in lower-closed canopy forest	Trees with greater ring width sensitivity may produce clearer hydroclimatic signal.
Beetle preferred trees	Canopy dominants larger than 40cm dbh	Trees in this size class are preferred by beetles during outbreaks

Table 8 - Model selection matrix. Model types include Random Forest (RF) and linear model (LM). For each subset, the rank for each of the ten most important variables are listed. NOTE: Due to bootstrap sampling in RF algorithms, slight changes in rank are common and expected when re-run. Linear models were fit using least squares regression and variables selection using AIC. Due to the large number of predictors, candidate variables in LMs were selected from the following subsets: Snowpack & melt variables, previous WY precipitation, same WY precipitation, previous WY temperature, same WY temperature. Variables retained through AIC selection with these groups were then passed on to a final model selection. Variable significant codes are: $p > 0.1$ (NS); $p < 0.1$ (+); $p < 0.05$ (*); $p < 0.001$ (**); $p < 0.0001$ (***). Variables with no code were removed from the model by AIC criteria. NOTE: the variable *Year* was included in each of the initial variable subset model selection runs to capture the normal trend of decreased growth with increasing age/size.

Subset of trees		**No subset, all trees**			**Most sensitive subset**			**Beetle-preferred subset**		
Model type		**RF**	**LM - initial**	**LM - Final**	**RF**	**LM - initial**	**LM - Final**	**RF**	**LM - initial**	**LM - Final**
Full Model	R^2_{adj} =	0.49		0.75	0.44		0.79	.48		0.77
Snowpack & melt variables	R^2_{adj} =		0.53			0.51			0.64	
	Year	1	**	+	1	+		1	***	**
	swemx_in	4			2	*		5		
	swemx_doy					NS				
	sag_doy									
	Melt_per									
	swemx_in.p	2	***	**	6	*		4	***	***
	swemx_doy.p									
	sag_doy.p							10		
	Melt_per.p									
	mod7resid									
	mod7resid.p		NS	NS					*	NS
Previous WY precipitation variables			0.44			0.44			0.61	
	Year	1			1			1	NS	
	ppt.01p									
	ppt.02p		**			**			***	*
	ppt.03p	10	**		4	***	NS		*	NS
	ppt.04p									
	ppt.05p							3		
	ppt.06p		**						**	
	ppt.07p					NS			+	+
	ppt.08p		*	+		*	**		**	NS
	ppt.09p		*	+		**	*		*	*

Table 9 - Continued

Subset of trees	No subset, all trees			Most sensitive subset			Beetle-preferred subset		
Model type	**RF**	**LM - initial**	**LM - Final**	**RF**	**LM - initial**	**LM - Final**	**RF**	**LM - initial**	**LM - Final**
Full Model R^2_{adj} =	0.49		0.75	0.44		0.79	.48		0.77
Same WY precipitation variables		0.44			0.57			0.52	
Year	1	***		1	*		1	***	
ppt.10p									
ppt.11p									
ppt.12p					+	**		NS	
ppt.01		+	+					+	
ppt.02									
ppt.03				9	+				
ppt.04		**	***	10	*	**		*	
ppt.05				8					
ppt.06	6			3	*	*			
ppt.07									
ppt.08		+			NS			*	
ppt.09		+	*					*	NS
Previous WY temperature variables		0.40			0.23			0.48	
Year	1	*		1	**		1	**	
tmean.01p									
tmean.02p									
tmean.03p									
tmean.04p		+						NS	
tmean.05p				10					
tmean.06p	7								
tmean.07p	3	*					2	*	
tmean.08p									
tmean.09p									
Same WY temperature variables		0.41			0.49			0.41	
Year	1			1			1	***	
tmean.10p									
tmean.11p									
tmean.12p		+			**	+			
tmean.01		NS						*	+
tmean.02				5					
tmean.03	8	*	**		**	***	8		
tmean.04		*	*	7	**	NS			
tmean.05		NS							
tmean.06							7		
tmean.07	9	**	*		**	**	9		
tmean.08									
tmean.09	5						6		

Whole forest: no subsetting

I found no strong relationships between ring width index and variables related to dust-on-snow effects. However, the snow-all-gone date for the water year of growth and the water year preceding growth showed the strongest correlations (Figure 15, top-left and bottom-left), both of which were positive in sign indicating that earlier snow-all-gone dates are associated with decreased annual growth.

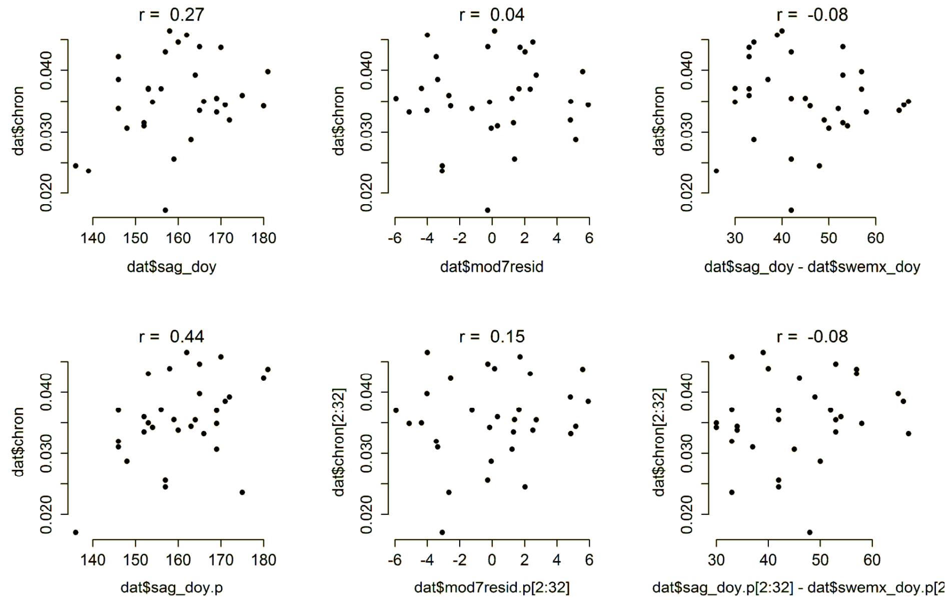

Figure 15 - Scatterplots of ring width index for all trees and hydroclimatic variables related to dust-on-snow effects. For variable names, see Table 3 and Table 4.

The model of annual growth using all trees sampled during the study included 243 ring width series from 122 trees. More than half (n=74) of these were canopy dominant trees.

The importance of variable *Year* indicates a long-term trend in the ring width index over time. Specifically, ring width decreases with age. This trend is expected since annual radial growth tends to decrease as trees become larger and older. In addition to the trend associated with *Year*, the Random Forest model importance metrics highlight six additional variables: *swemx_in.p, tmean.07p, swemx_in, tmean.09, ppt.06, and tmean.06*. These variables indicate that total snowpack, early summer temperature and precipitation during the short dry season (June) are the most important determinants of ring width variability. The relationship with June precipitation is particularly interesting and suggests a non-linear or threshold effect. While precipitation amounts greater than two inches seems to cause little or no change in ring width, below two inches ring width index values drop off sharply (Figure 17). Variables relating to DOS were not identified by the Random Forest model as being important variables explaining variations in ring width. Overall, the Random Forest model was not able to produce as good a fit to the data compared with linear models (Table 8).

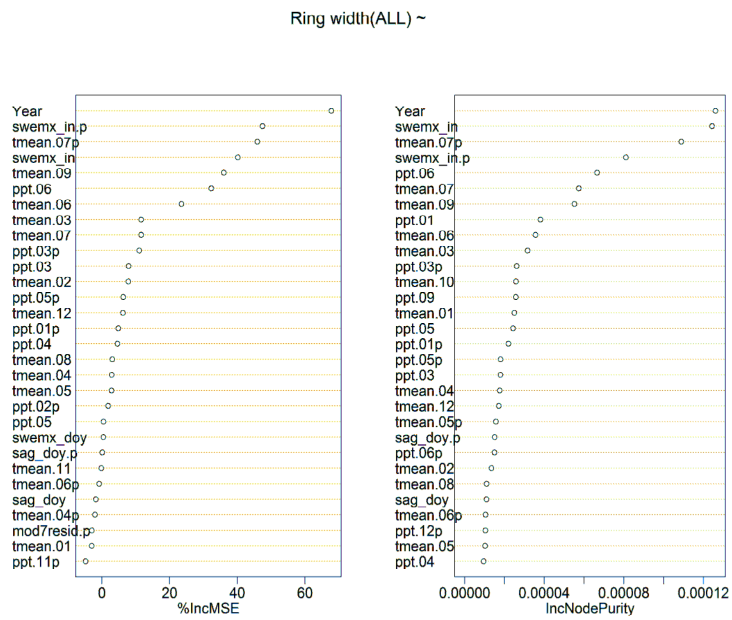

Figure 16 - Variable importance metrics for a Random Forest model of ring width index as a function of many hydroclimatic variables. The ring width index was produced from a chronology of 243 ring width series spanning years 1981-2012 from 122 trees in the Senator Beck Basin, Red Mountain Pass, CO.

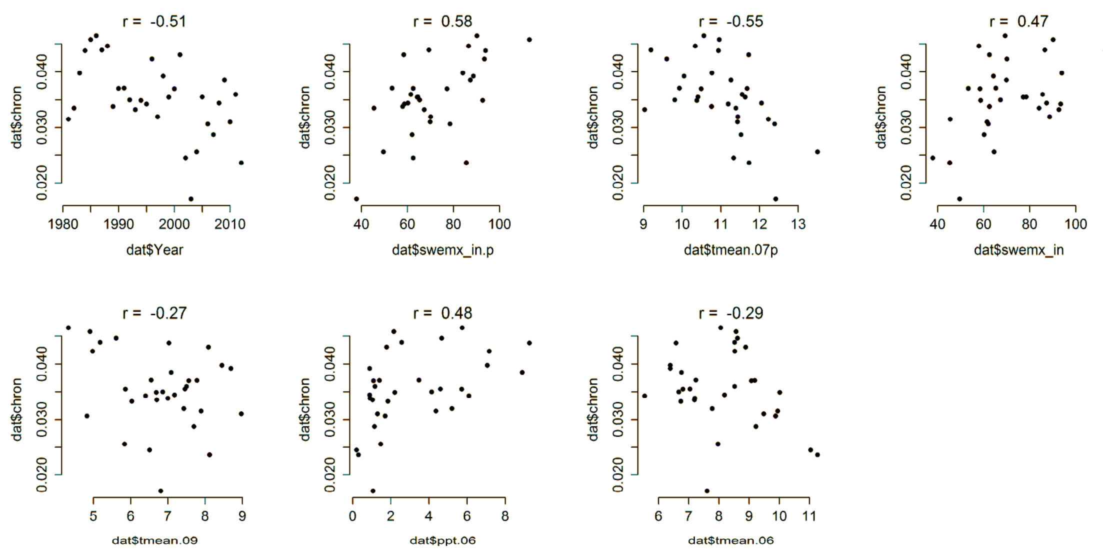

Figure 17 - Scatterplots showing relationships between ring-width index and important hydroclimatic variables.

The linear model of ring width index included many of the same or similar variables. Again, Year was found to be important, as was snowpack amount for the previous water year. The importance of March and July temperatures for the WY of growth was consistent across models. For both of these, the relationship is negative indicating that warm temperatures negatively impact growth. Total SWE amount for the previous WY was also consistently important for explaining variation in ring width. For the linear model, AIC criteria suggest that SAG model residuals for the previous WY are informative and should be retained in the full and final model, however the coefficient estimate for this parameter was not significantly different from zero which weakens the case for its importance.   Together, these data suggest that, forest-wide, tree ring width is most

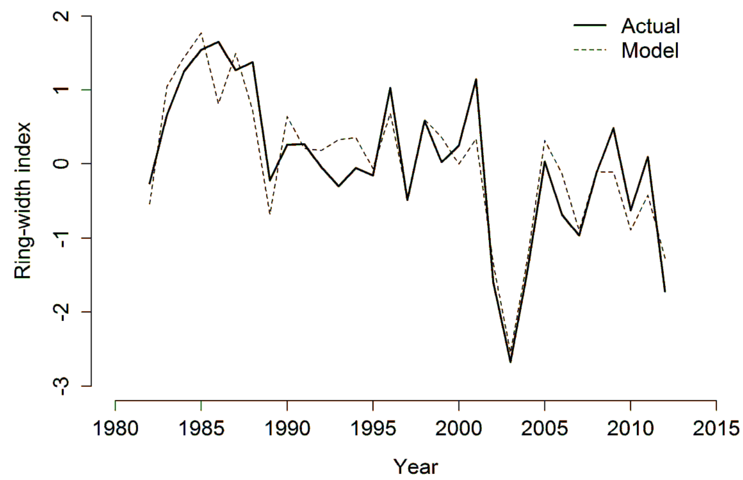

Figure 18 - Plot of observed (solid) and modeled (dashed) ring-width index for a chronology of 243 tree ring series (122 trees) in the Senator Beck Basin, Red Mountain Pass, CO. All series span the time period 1982-2013.

Table 10 – Estimates and statistics for standardized coefficients of the final (linear) model of ring width index for all trees as a function of hydroclimatic variables.

Coefficients:					
	Estimate	Std.	Error	t	Pr(>|t|)
(Intercept)	-0.00051	0.091447	-0.006	0.995625	
Year	-0.28639	0.144695	-1.979	0.062461	.
swemx_in.p	0.36333	0.105589	3.441	0.002738	**
mod7resid.p	0.149414	0.100062	1.493	0.151802	
ppt.08p	0.195492	0.108492	1.802	0.087451	.
ppt.09p	0.180159	0.09881	1.823	0.084034	.
ppt.01	0.186869	0.105028	1.779	0.091205	.
ppt.04	0.534803	0.136839	3.908	0.000945	***
ppt.09	-0.23052	0.102115	-2.257	0.035947	*
tmean.03	-0.3614	0.118944	-3.038	0.006761	**
tmean.04	0.280155	0.133844	2.093	0.049987	*
tmean.07	-0.3176	0.120595	-2.634	0.016366	*

Subset: Most sensitive trees

The trees showing the most year-to-year variation in ring width are canopy subdominants in forests with a lower closed canopy structure (see section *Tree-ring sensitivity*, above). I created a ring width index using a small subset of the full dataset, just 13 series from a total of 7 trees that were classified in the field as CS and LCL.

As with the full dataset, hydroclimatic variables relating to DOS effects did not correlate strongly with this index (Figure 19).

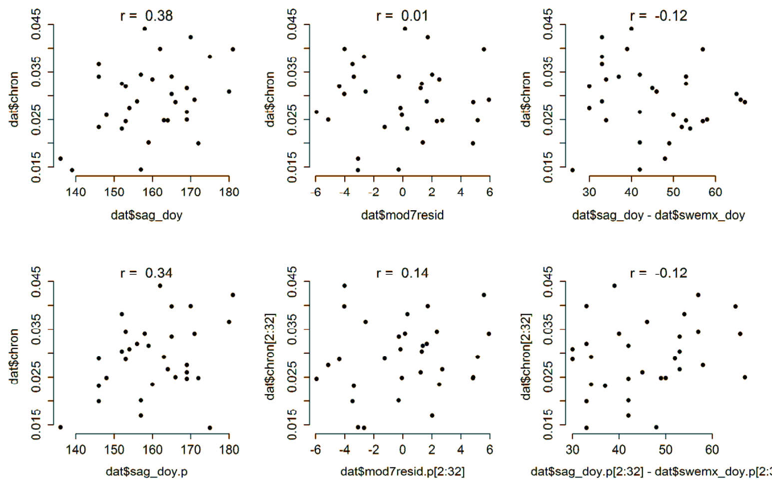

Figure 19 - Scatterplots of ring width index for all trees and hydroclimatic variables related to dust-on-snow effects. For variable names, see Table 3 & Table 4.

Similar to the model using all trees, this subset Random Forest model was not able to produce a good fit to the data. Using just the seven most important variables, the Random Forest model was able to explain only a moderate amount (44%) of the total variance.

Variable importance metrics (Figure 20) from the RF model highlight the influence of snowpack, springtime precipitation and June precipitation on annual growth. There also appears to be a moderate positive association with February temperatures.

The full final linear model explains 79% of the variance in ring width. As with the previous (all trees) model, late summer precipitation during the previous water year was found to be important, as was spring (March & April) and summer (July) temperatures.

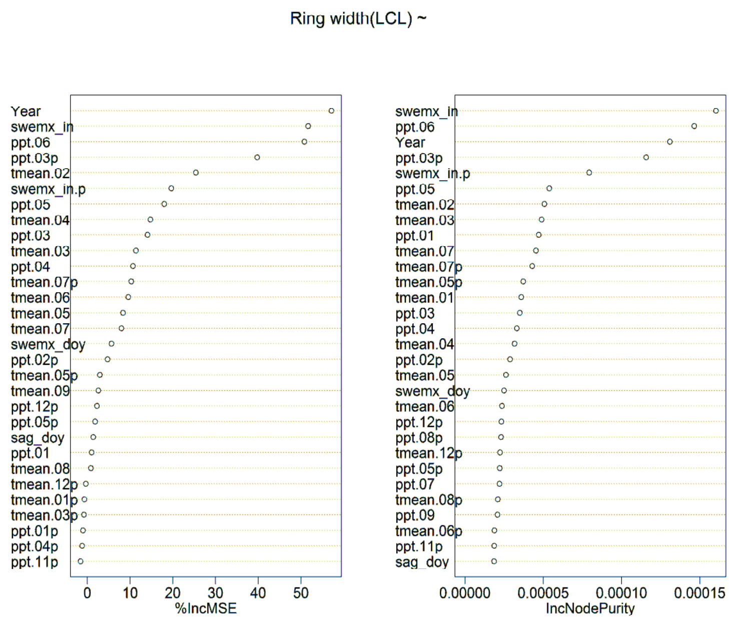

Figure 20 - Variable importance ranking output from a Random Forest model of mean annual ring width among canopy subdominant (cs) trees located in a lower closed canopy (lcl) forest in the Senator Beck Basin, Red Mountain Pass, CO, USA. Data are from the period 1982-2013.

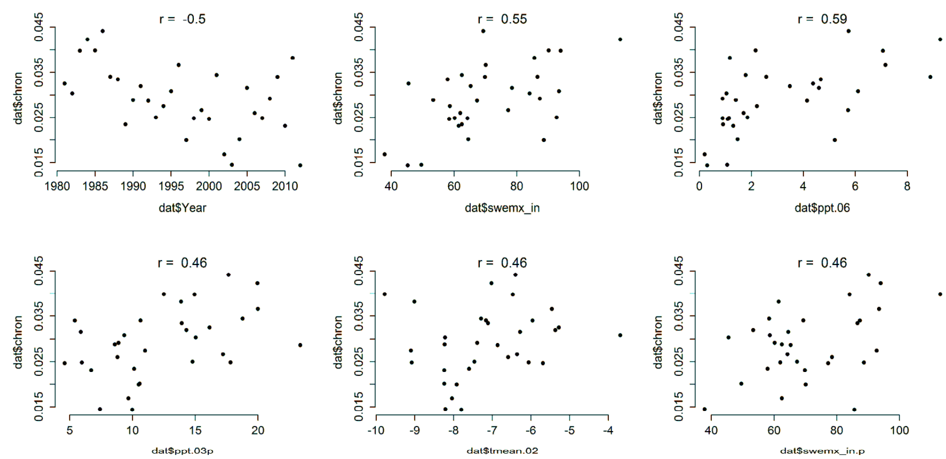

Figure 21 - Scatterplots of ring width index for the canopy subdominant, lower closed canopy structure subset and important hydroclimatic variables identified using a Random Forest model.

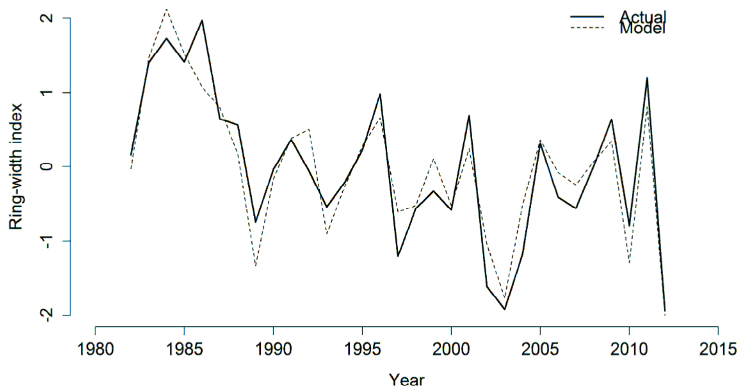

Figure 22 - Plot of actual (solid) and modeled (dashed) ring-width index for 13 tree ring series (7 trees), each spanning the time period 1982-2013.

Table 11 - Estimates and statistics for standardized coefficients of the final (linear) model of ring width index as a function of hydroclimatic variables. Ring width index is for the most sensitive subset of trees.

Coefficients:					
	Estimate	Std.	Error	t	Pr(>|t|)
(Intercept)	-0.00041	0.085411	-0.005	0.99621	
ppt.03p	0.162515	0.106997	1.519	0.14444	
ppt.08p	0.256895	0.090206	2.848	0.00994	**
ppt.09p	0.254061	0.100959	2.516	0.0205	*
ppt.12p	0.313944	0.094037	3.339	0.00327	**
ppt.04	0.435881	0.1272	3.427	0.00267	**
ppt.06	0.24958	0.119325	2.092	0.04944	*
tmean.12p	0.271141	0.134662	2.013	0.05772	.
tmean.03	-0.54394	0.102873	-5.288	3.56E-05	***
tmean.04	0.19199	0.136842	1.403	0.17595	
tmean.07	-0.30184	0.101134	-2.985	0.00733	**

Subset: Beetle-preferred trees

During large outbreaks, beetles seek out large, dominant trees to attack. These trees contain a cambium layer that is more nutrient rich and supports larger broods compared with smaller, weaker trees. I modeled ring width using hydroclimatic variables for the subset of trees that are canopy dominants and larger than 40 cm in diameter at chest height.

Correlation with DOS metrics was slightly stronger for the beetle-preferred subset, at least for the SAG date during the previous WY.

The Random Forest variable importance metrics (Figure 24) suggest that summer temperatures and snowpack volume are the most important determinants of ring width variation. These results generally agree with the previous models.

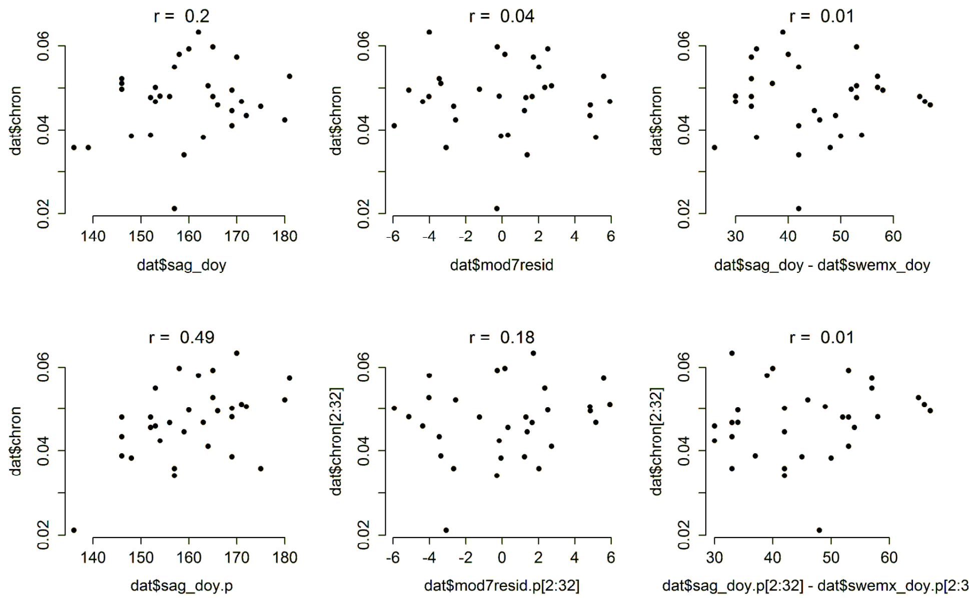

Figure 23 - Scatterplots of ring width index for beetle-preferred trees and hydroclimatic variables related to dust-on-snow effects. For variable names, see Table 3 & Table 4. Variable mod7resid is the unexplained variance in snow-all-gone day of year (see Snow-all-gone section, above). Variable mod7resid.p is for the previous water year. The plots furthest right show melt period for the same WY of growth (top) and previous WY (bottom), which is the SAG date minus the peak swe date.

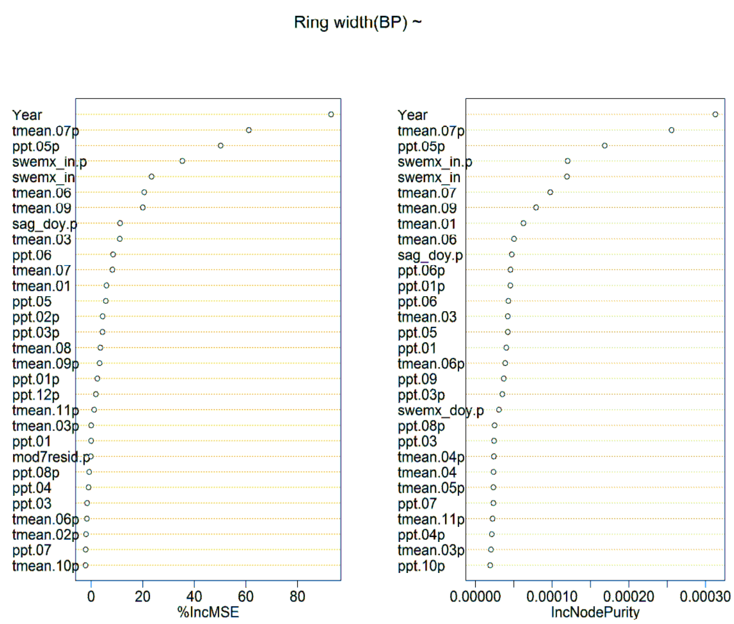

Figure 24 - Variable importance ranking output from a Random Forest model of mean annual ring width among beetle-preferred trees in the Senator Beck Basin, Red Mountain Pass, CO, USA. Data are from the period 1982-2013.

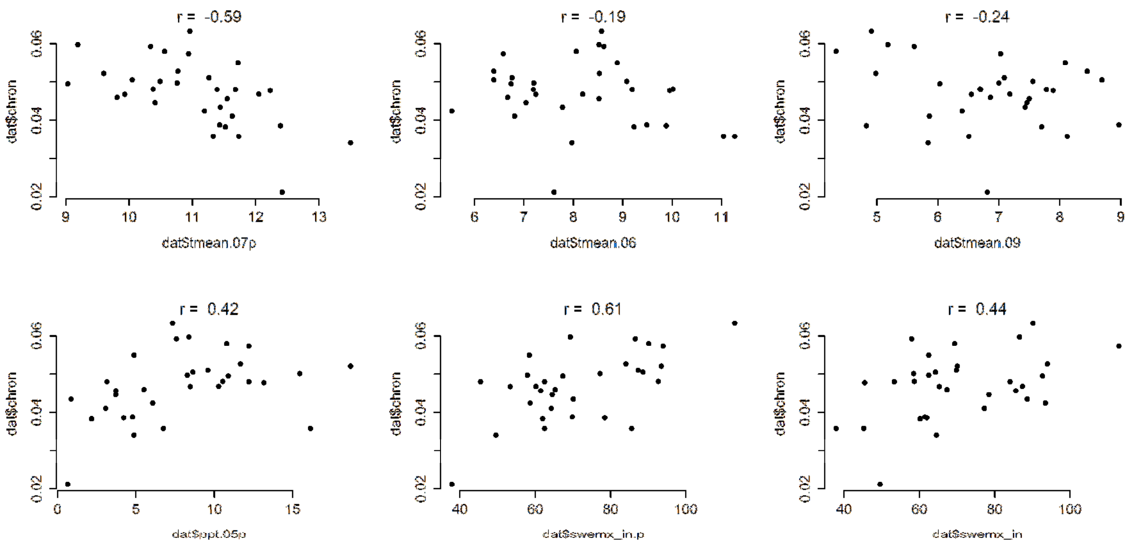

The full and final linear model for ring width of this subset indicates that previous WY snowpack, and precipitation in general, is strongly associated with variation in ring width. Unlike the "all trees" and "sensitive trees subset" models, associations with temperature are practically non-existent in this model. This also contrasts with the Random Forest model for the same data. Another difference is the significance given to *Year* as a variable. While declining ring width overtime is expected in tree-ring series, the weight given to the year effect (standardized coefficients represent magnitude of effect) for such a short period of time (~30 years) suggests that perhaps some other trend over time exists in the data that is enhancing the decrease in ring widths over time. A look at the temperature data (Figure 25) show a gradual warming trend in spring and summer temperatures. Because monthly and not seasonal data were used, such a trend could not be attributed correctly to any "tmean" variable and would show up as a trend over time (ie. *Year*). Similarly, dust deposition has been increasing for at least the past 17 years (Brahney et al. 2013).

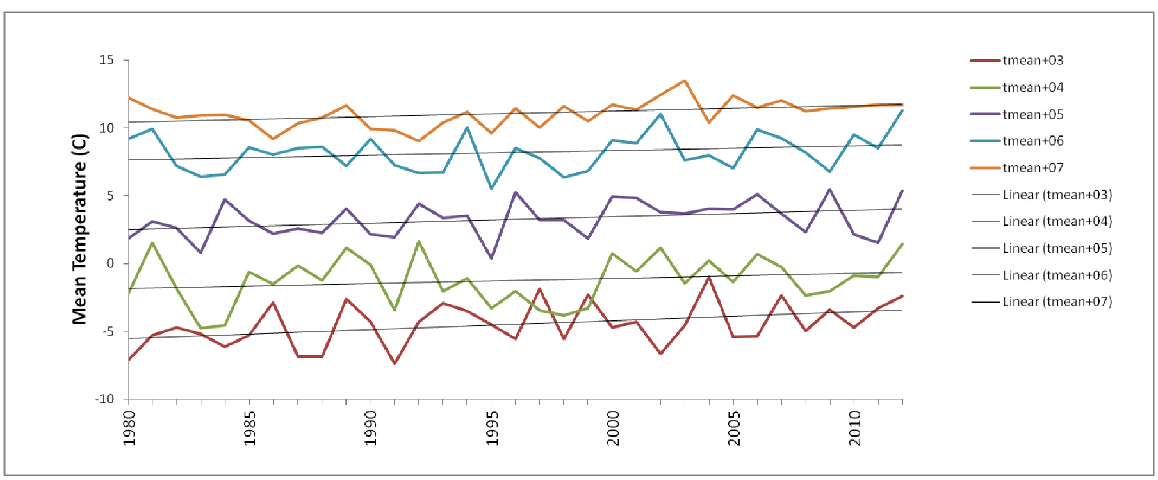

Figure 25 – Spring and summer month temperatures for the period 1980-2012. Months shown are March through July. Data are from the PRISM climate data set centered on Red Mountain Pass, CO.

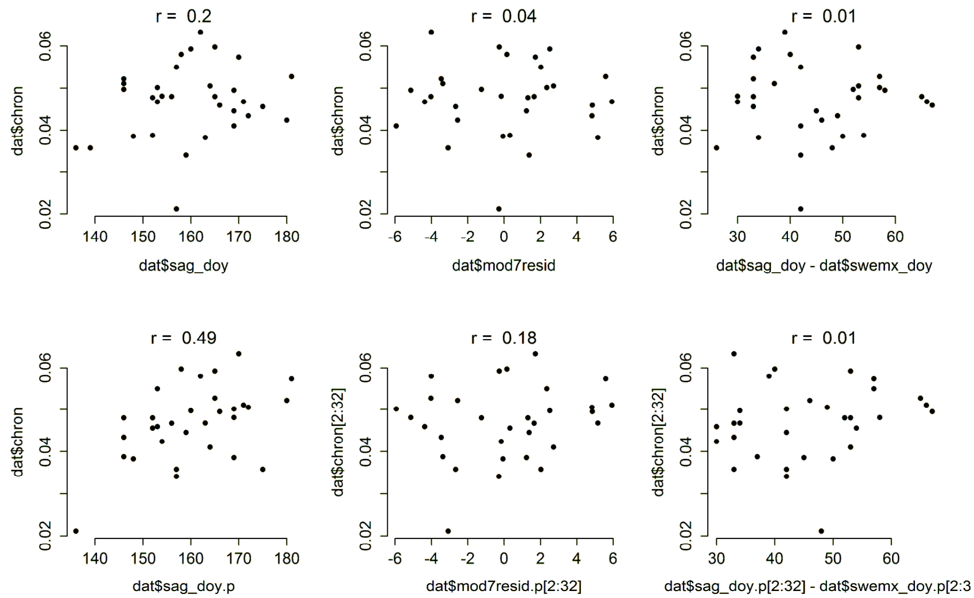

Figure 26 - Scatterplots of ring width index for the beetle-preferred trees subset and important hydroclimatic variables identified using a Random Forest model.

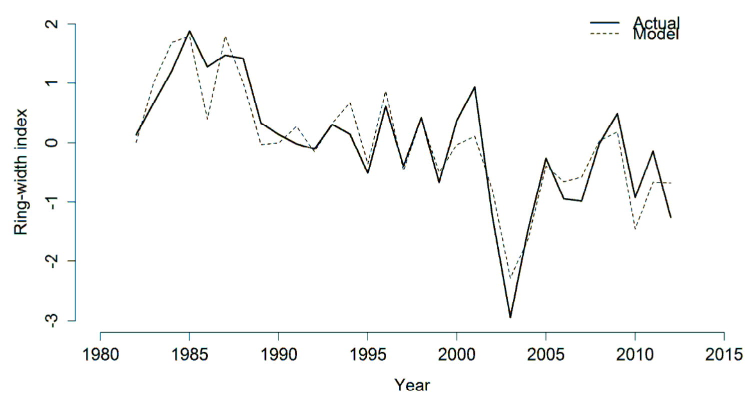

Figure 27 - Plot of actual (solid) and modeled (dashed) ring-width index for 13 tree ring series (7 trees), each spanning the time period 1982-2013.

Table 12- Estimates and statistics for standardized coefficients of the final (linear) model of ring width index as a function of hydroclimatic variables. Ring width index is for beetle-preferred trees, which are canopy dominant trees 40ccm dbh or larger.

Coefficients:					
	Estimate	Std.	Error	t	Pr(>|t|)
(Intercept)	-0.00491	0.090239	-0.054	0.957171	
Year	-0.36274	0.119623	-3.032	0.006578	**
swemx_in.p	0.434094	0.107975	4.02	0.000671	***
mod7resid.p	0.152962	0.096793	1.58	0.129723	
ppt.02p	0.353631	0.130235	2.715	0.013323	*
ppt.03p	0.182608	0.10791	1.692	0.106126	
ppt.07p	0.206389	0.10015	2.061	0.052566	.
ppt.08p	0.17497	0.108077	1.619	0.121124	
ppt.09p	0.25546	0.104339	2.448	2.37E-02	*
ppt.09	-0.16034	0.093944	-1.707	0.103343	
tmean.01	-0.23552	0.119318	-1.974	0.062369	.

Conclusions

While the influence of DOS effects on tree growth cannot be ruled out, the magnitude of any DOS effect is probably very small relative to variables such as snowpack volume and growing season temperatures. However, the snowmelt metrics used in this study come from a single location whereas the tree ring data come from several locations with varying aspects, forest structures, stand densities and proximity to surface flow. Because shading by terrain and vegetation play key roles in the energy input and melting of snowpack, the snowmelt data used in this study may not be representative of the conditions experienced by trees sampled on sunnier locations. It is possible that snowmelt data collected from more extreme locations (south-facing with open forest) would have correlated more strongly with tree ring data collected from trees on sunnier, more open aspects.

Perhaps the most interesting finding in this study relates to the degree with which trees in SBB show sensitivity to moisture stress. Conventional thinking suggests tree growth at high elevations (such as those in the SBB) is more strongly influenced by growing season length than moisture deficit. The data in this study suggest high elevation trees may show sensitivity to moisture stress especially sub-dominant trees located in dense, relatively closed forest.These data do not suggest that tree growth increases with warmer temperatures, a notable exception being during April, but ratherthat warmer temperatures and drier conditions are associated with decreased growth. However, canopy dominant trees appear less sensitive overall compared with sub-dominants. An explanation for this might be that in drier years, competition for water is more intense and dominant trees are stronger competitors and able to capture more of the resources they need relative to sub-dominant trees.

If trees in the SBB are showing sensitivity to moisture stress, it is not unreasonable to think that faster snowmelt would increase competition and result in moisture stress among at least some part of the population. However, the magnitude of this DOS effect appears small compared to the effect of exceptionally warm, dry years—like 2002, 2003, 2012—regardless of DOS effect. And while DOS may exacerbate moisture stress during periods of drought, the effect of the drought alone is very large as indicated by the strong correlations between ring width and SWE amount and the large coefficient for SWE amount in the linear models.

Abràmoff, M. D., P. J. Magalhães, and S. J. Ram. 2004. Image processing with ImageJ. Biophotonics international **11**:36-43.
Brahney, J., A. P. Ballantyne, C. Sievers, and J. C. Neff. 2013. Increasing Ca2+ deposition in the western US: The role of mineral aerosols. Aeolian Research **10**:77-87.
CODOS (Colorado Dust-on-Snow Program). 2014. Center for Snow and Avalanche Studies, Silverton, CO. http://www.codos.org/#codos
Steltzer, H., C. Landry, T. H. Painter, J. Anderson, and E. Ayres. 2009. Biological consequences of earlier snowmelt from desert dust deposition in alpine landscapes. Proceedings of the National Academy of Sciences **106**:11629-11634.
Skiles, S. M., T. H. Painter, J. S. Deems, A. C. Bryant, and C. Landry (2012), Dust radiative forcing in snow of the Upper Colorado River Basin: Part II. Interannual variability in radiative forcing and snowmelt rates, *Water Resour. Res.*, doi:10.1029/2012WR011986.
Stokes, M. A., and T. L. Smiley. 1968. An introduction to tree-ring dating. University of Chicago Press.

Location coordinates

ident	Latitude,N	Longitude	y_proj	x_proj
SBB01	37.909485	-107.707915	-1114421.6898722	5009105.20191292
SBB02	37.910071	-107.709046	-1114260.60017112	5008747.70542686
SBB03	37.909918	-107.708693	-1114300.06191537	5008857.58523165
SBB04	37.909354	-107.708203	-1114482.05208811	5009030.09225092
SBB05	37.910693	-107.709598	-1114060.41535226	5008554.1343745
SBB06	37.911238	-107.710987	-1113925.7650148	5008125.02359974
SBB07	37.912134	-107.712	-1113647.19363941	5007783.75379957
SBB08	37.902519	-107.713423	-1117189.93322468	5007922.05323974
SBB09	37.904661	-107.717167	-1116583.44736488	5006727.0766932
SBB10	37.90754	-107.710072	-1115222.49452682	5008597.41961228
SBB11	37.90558	-107.711991	-1116018.00476491	5008158.67677356